

Impact of earthquake rupture extensions on parameter estimations of point-process models

S. Hainzl¹, A. Christophersen², and B. Enescu¹

¹ *GeoForschungsZentrum Potsdam, Germany;* ² *Swiss Seismological Service, ETH Zürich, Switzerland*

Abstract

Stochastic point-processes are widely applied to model spatio-temporal earthquake occurrence. In particular, the ETAS (Epidemic Type Aftershock Sequence) model has been shown to reproduce successfully the short-term clustering of earthquakes. An important parameter of the model is the α -value describing the scaling of the aftershock productivity with magnitude of the triggering earthquake according to $10^{\alpha M}$. Fitting of the space-dependent ETAS model to empirical data yields α -values which are typically much smaller than the scaling inverted from more simple stacking of aftershock sequences. We show by means of synthetic simulations that this is likely to result from assuming spatial isotropy of aftershock occurrence which in fact aligns along the mainshock rupture. We fit the space-dependent and independent ETAS models to simulations where each earthquake is a line source with an empirical magnitude-length relation. Although the space-time model describes past activity quite well, it overestimates the forecasted earthquake rate. On the other hand, the application of the space-independent ETAS predicts future seismicity well and can therefore be applied for forecasting purposes. Our test for the observed aftershock sequence following the 1992 M7.3 Landers earthquake supports these results.

1 Introduction

In the recent past, strong efforts have been undertaken to test our present-day ability to forecast earthquakes, e.g. within the RELM (Hough and Olsen, 2007) and the CSEP-projects (<http://sceccdata.usc.edu/csep>). Within this context, the forecasting of aftershocks is also of interest (e.g. Gerstenberger et al., 2005, and SAFER-project: <http://www.saferproject.net/index.htm>). Forecasting of aftershocks seems to be feasible because of two well-known empirical laws: (1) The aftershock rate generally decays according to the Omori-Utsu law, $\sim (c + t)^{-p}$, where c and p are constants, and t is the elapsed time since the main event (for a review see Utsu et al., 1995); and (2) the aftershock area grows exponentially with mainshock magnitude M (Utsu and Seki, 1955) and so does the number of aftershocks (Kanamori and Anderson, 1975), leading to the productivity proportional to $10^{\alpha M}$.

The Epidemic Type Aftershock Sequence (ETAS) model is a stochastic point process model that builds on the above mentioned empirical characteristics and takes stationary seismicity and secondary aftershocks into account (Ogata, 1988; Helmstetter and Sornette, 2002). In the ETAS model, each earthquake has some magnitude M dependent ability to trigger aftershocks according to $K 10^{\alpha(M - M_{min})}$ where K is a constant and M_{min} is the lower magnitude cutoff of the earthquakes under consideration. In this context and throughout the whole paper, aftershocks are defined as triggered events independent of whether they are smaller or larger than their parent earthquakes.

The total occurrence rate of earthquakes is given by

$$\lambda(t, x, y) = \mu + \sum_{i:t_i < t} \frac{K 10^{\alpha(M_i - M_{min})}}{(t - t_i + c)^p} f_i(x - x_i, y - y_i) \quad (1)$$

with μ being the background rate and $f_i(x, y)$ a normalized function, which describes the spatial probability distribution of triggered aftershocks. Frequently, the isotropic power-law kernel

$$f(x, y) = \frac{(q - 1) d^{2(q-1)}}{\pi [x^2 + y^2 + d^2]^q} \quad (2)$$

is used with the two parameters q and d (Console et al., 2003; 2006; Zhuang et al., 2004; Helmstetter et al., 2005). A q -value of 1.5 would be consistent with static stress triggering, which decays according to $\sim r^{-3}$. To account for anisotropy, a more general form was originally proposed by Ogata (1998) where $x^2 + y^2$ is replaced by $(x, y) \mathbf{S} (x, y)^t$. Here \mathbf{S} is a 2×2 positive definite symmetric matrix, and $(x, y)^t$ indicates the vector transpose relative to the centroid of the aftershock cloud. The quadratic form allows aftershocks to be spatially distributed with ellipsoidal contours. However, as the inversion of \mathbf{S} from earthquake data is not straightforward because in general \mathbf{S} and the centroid position must be estimated for each event independently, an identity matrix is usually assumed leading to Eq.(2).

A number of studies have addressed how the number of aftershocks produced by a mainshock depends on its magnitude (Kanamori and Anderson, 1975; Yamanaka and Shimazaki, 1990; Felzer et al., 2002, 2004). While there is good evidence that the productivity grows exponentially with M as $\sim 10^{\alpha M}$, the exact value of α varies substantially between empirical studies, in particular, between windows-based cluster definitions and ETAS-model fits. Although Christophersen and Smith (2008) showed that the inferred α -value depends on the applied magnitude-scaling of the spatial windows, the former class yields typically values close to 1: Helmstetter (2003) obtained that $0.7 < \alpha < 0.9$ for southern California, while Helmstetter et al. (2005) found $\alpha = 1.05 \pm 0.05$, for the same region. An α -value close to 1 would imply that the number of aftershocks scales in a similar way as the mainshock rupture area. This is also in general agreement with the scattered α -values around 1, which are obtained by the space-independent ETAS model ($f(x, y)=1$) for various sequences in Japan (Ogata, 1992). On the other hand, using space-dependent ETAS models and inverting for the model parameters yields significantly lower values, e.g., Zhuang et al. (2004) found that $\alpha \simeq 0.6$ for Japan (1926-1999 $M \geq 4.2$ earthquakes), Zhuang et al. (2005) found $\alpha = 0.7 \pm 0.05$ for Taiwan (1941-2001 $M \geq 5.3$ earthquakes), while Console et al. (2003) obtained $\alpha = 0.42$ for Italy (1987-2000 $M \geq 2$ earthquakes).

In this study, we show that the apparently smaller values inverted by means of the space-time ETAS models are likely to result from neglecting the earthquake rupture extensions because earthquakes are treated as point-sources with a spatially isotropic probability function for aftershock triggering. If the spatial extent of earthquake sources is not taken into account, forecasting of ongoing aftershock activity is erroneous. To show this, we will analyze ETAS simulations with realistic spatial aftershock distribution in Section 2 and study the Landers aftershock sequence in Section 3.

2 Synthetic Simulations

We used Monte Carlo simulations of the ETAS model as described by equations (1) and (2). To choose appropriate input parameters for these simulations, we fitted the ETAS model to the seismicity preceding the 1992 M7.3 Landers, California, earthquake. We used the relocated data

set by Hauksson et al. (2003) for the region -119W to -115.5W and 32.5N to 36.5N and the time interval between $t_1=1/1/1984$ and $t_2=6/27/1992$ (downloaded from the SCEDC webpage at <http://www.data.scec.org/research/altcatalogs.html>). The catalog included $N=1537$ earthquakes with magnitude $M \geq 3$. We optimized the parameters μ, K, c, p, q and d by maximum likelihood method which is performed according to Ogata (1992), using the Davidon-Fletcher-Powell method (e.g., Fletcher and Powell (1963)). The α -parameter was thereby set to the middle of previous estimations, $\alpha=0.8$. As discussed later, a free α would have been underestimated by the space-dependent ETAS model.

The likelihood function can be written as

$$\begin{aligned} \ln L &= \sum_{i=1}^N \ln \lambda(t_i, x_i, y_i) - \int_{t_1}^{t_2} \int_{x_1}^{x_2} \int_{y_1}^{y_2} \lambda(t, x, y) dx dy dt \\ &= \sum_{i=1}^N \ln \lambda(t_i, x_i, y_i) - \mu(x_2 - x_1)(y_2 - y_1) - \int_{t_1}^{t_2} \sum_{i:t_i < t} \frac{K 10^{\alpha(M_i - M_{min})}}{(t - t_i + c)^p} dt \end{aligned} \quad (3)$$

(Ogata, 1998; Daley and Vere-Jones, 2003). The inverted values are summarized in table 1. Note that for the simulations, we set the background rate to 0 instead of the inverted small value of 0.039 [day⁻¹].

| $M_{main}(t=0)$ | M_{min} | μ [day ⁻¹] | K | c [days] | α | p | q | d [km] |
|-----------------|-----------|----------------------------|--------|------------|----------|------|------|----------|
| 7.3 | 3.0 | 0 | 0.0157 | 0.0016 | 0.8 | 0.99 | 1.45 | 0.53 |

Table 1: Summary of the model input parameters for the ETAS simulations.

We produced Monte Carlo simulations of the ETAS model using the inverse (transform) method (see e.g. Daley and Vere-Jones, 2003). A mainshock of magnitude 7.3 was assumed to occur at time 0. Aftershock magnitudes were drawn from a Gutenberg-Richter frequency-magnitude distribution with $b=1$ and a maximum magnitude of 7.0. To account for the spatial extension of each rupture, we assumed that the rupture length L scales with the earthquake magnitude according to the empirical relation of Wells and Coppersmith (1994): $L = \sqrt{A} = \sqrt{10^{-3.49+0.91M}}$ [km] (where A is the rupture area) and took the form of a line with random orientation in space. Each point on the rupture could equally trigger aftershocks according to the isotropic kernel. This was done by firstly selecting a random point on the rupture (line segment) and then selecting a random point relative to this location according to the spatial probability function of Eq.(2). An example for such a simulated aftershock sequence is shown in Fig.1 in comparison to the Landers aftershock sequence.

We analyzed the Monte-Carlo simulations with two different inversion strategies: (A) Inversion by means of the space-time ETAS model, and (B) inversion by the space-independent model. In the latter case, Eq.(2) is replaced by $f(x, y)=1$.

At first, we investigated whether the input parameters can be obtained by maximizing the likelihood function (Eq.3). For 100 simulations, Fig.2 shows the results for the inversion of the first 10 days of aftershocks (typically about 1000 events). The results are striking: The procedure (B) which neglected all information about the spatial triggering results in an unbiased estimation of all parameters ($K = 0.015 \pm 0.002$, $c = 0.0017 \pm 0.0004$ days, $\alpha = 0.81 \pm 0.02$, $p = 0.99 \pm 0.02$). By contrast, procedure (A) which used the correct model besides the fact that earthquakes were taken as point-sources leads to significantly wrong estimations. In particular, the parameter $K = 0.037 \pm 0.002$ is estimated significantly too high and $\alpha = 0.55 \pm 0.02$ too low. Note that both parameter

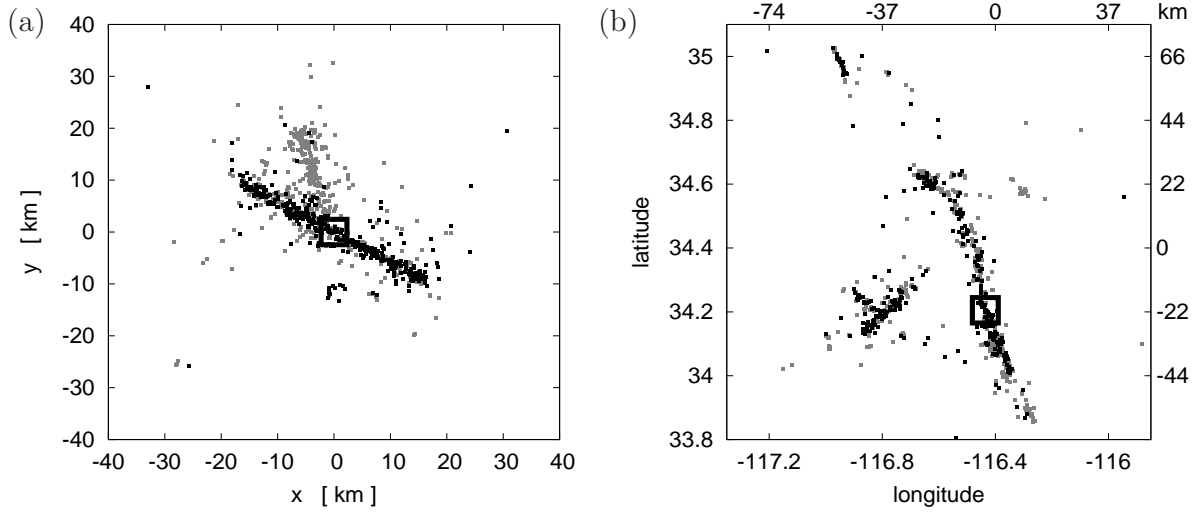


Figure 1: (a) Example of an ETAS simulation; (b) Landers aftershocks. Both plots show all $M \geq 3$ aftershocks occurred within the first 10 days, where the aftershocks of the first 24 hours are plotted in black. In each plot, the epicenter of the mainshock is additionally marked by a big square.

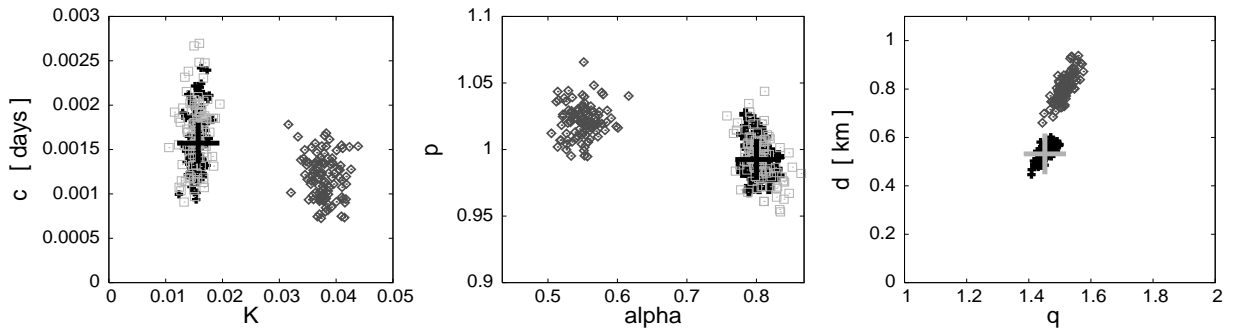


Figure 2: Estimated parameters by fitting the space-dependent (diamonds) and independent (squares) ETAS models to the first 10 days of aftershocks for 100 different stochastic simulations. The true values are indicated by the large crosses. For comparison, the test results for simulations with isotropic aftershock distributions are additionally shown for the space-dependent ETAS model (small black crosses, partially overlaid by the squares). In this case, the model yields unbiased estimations.

estimations are not independent but highly correlated. A tradeoff between both parameters is expected because the number of events is increasing rapidly for lower magnitude levels (according to the Gutenberg-Richter relation $N \sim 10^{-bM}$). If α becomes lower, then the more frequent smaller events contribute significantly more to the aftershock productivity and K must be smaller to result in the same total (observed) number of events.

We performed a test with simulations where we use point instead of line-sources for each earthquake. This test shows that the parameter mismatch is only due to the anisotropy of the aftershock clouds. As already suggested as one possibility by Helmstetter et al. (2006), the explanation is that a smaller α -value gives more importance to secondary aftershocks in the isotropic space-time ETAS model, and thus, the model can better adapt to the anisotropic, spatially elongated seismicity distribution triggered by the mainshock.

As presented in the electronic supplement material, we performed additional tests concerning the robustness of these results. Although we cannot perform an exhaustive testing of all possibilities which might have impact on the α -estimation (see discussion by Helmstetter et al. (2006)), our analysis indicates that neither the magnitude range, nor observational errors, nor spatial heterogeneities of the background activity affect the parameter estimation significantly. It is, however, found that using an isotropic spatial kernel (Eq.2) where d is scaling with the mainshock magnitude leads to a slightly better estimation than assuming a constant d -value. This agrees in principle with the observation that estimates with variable $d(M)$ lead to higher α -values (Zhuang et al., 2004) than those with constant d (Console et al. 2003).

Forecasting ability

We now show that the forecasting ability is strongly affected if the anisotropy of aftershock clouds is ignored. We estimated the ETAS parameters from the aftershocks of the first $T=1$ day, 1 week and 1 month and used the inverted parameters to forecast the expected number of events for the subsequent N days. The forecasts were done again by Monte-Carlo simulations: For each inverted parameter set and given precursory activity, we calculated the average number of events which are simulated for the next N days in 10^4 different stochastic realizations. In the simulations, we took into account aftershocks of aftershocks triggered within the prediction period, which are known to significantly contribute to the overall rate in the ETAS model (Helmstetter et al., 2003). The ratio between forecasted and real number of earthquakes is shown in Fig. 3 together with its standard deviation. It can be clearly seen that while the space-independent approach leads to good forecasts (ratios ≈ 1), the space-dependent measurements overestimate the earthquake rates largely. In particular, the ratio of forecasted and observed events grows exponentially with time for parameter estimation following shortly after the mainshock. And even parameter estimations 30 days after the mainshock still yield forecasted rates more than twice the observations.

Besides the temporal predictability, we also tested the spatial forecasting ability. We applied three different procedures:

1. using the space-time ETAS model for inversion and prediction.
2. using the the space-independent ETAS model for the inversion of K, c, α , and p . The spatial triggering was twofold. Aftershocks were allowed to spatially trigger secondary aftershocks according to Eq.(2), where the two parameters q and d were taken from the estimates of the space-time ETAS model. The direct aftershocks of the mainshocks were assumed to be triggered on a spatial probability map, which resulted from smoothing of the first 0.1 days of aftershocks (a minimum number of 50 events) by means of

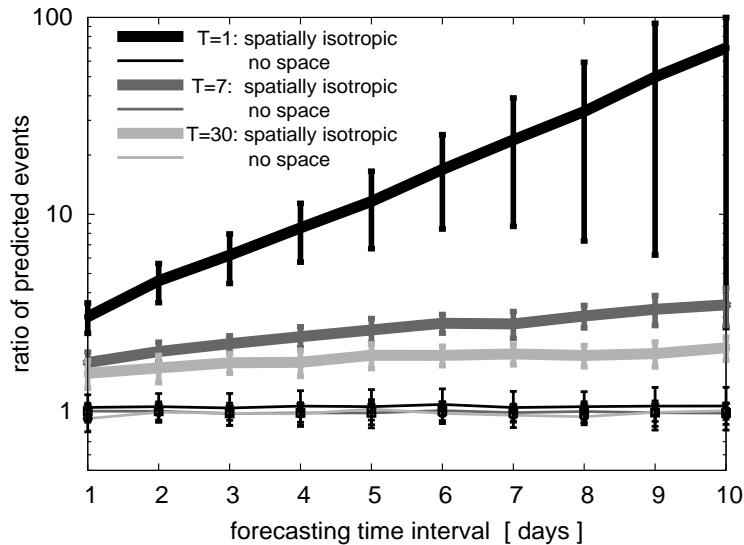


Figure 3: The ratio between the forecasted versus the true number of events as a function of the prediction time. The curves show average values together with their standard deviation for the space-dependent and space-independent ETAS models for different starting times T of the forecasts.

- (a) an isotropic adaptive Gaussian kernel according to Helmstetter et al. (2007), where we chose two neighbors for calculating the standard deviation.
- (b) the power-law kernel in Eq.(2) with inverted parameters q and d .

We calculated the coefficient r of the linear, spatial correlation between the estimated \tilde{p}_i and true p_i probability values at the N grid points in a 100 km \times 100 km box surrounding the mainshock (with grid-spacing of 1km) after 1 day, 5 days and 10 days. Mathematically, it is defined as $r = \frac{\sum_i^N (\tilde{p}_i - \langle \tilde{p} \rangle)(p_i - \langle p \rangle)}{N\sigma_{\tilde{p}}\sigma_p}$, where $\langle \rangle$ and σ_p denote the spatial average and standard deviation, respectively. The result, which is not significantly depending on the grid-spacing, is shown in Tab.2 for 100 different ETAS simulations. All three procedures led to comparable high correlations. Although the procedure 2b led to slightly better median values, this procedure as well as 2a sometimes had quite bad estimations which is reflected in the larger standard deviations. These were caused by large aftershocks with non-negligible rupture extensions. To improve the estimation, secondary large aftershocks must therefore also be treated similarly to the mainshock. However, this would lead to a complex algorithm with additional parameters (a magnitude cutoff to define the lower bound for smoothing; the time interval for smoothing; and a minimum event number for smoothing, see e.g. Helmstetter et al. 2007). Thus the straightforward and robust prediction of the spatial distribution by means of the space-time ETAS model (procedure 1) seems to be superior.

3 Landers Aftershock Sequence

Finally we applied the same procedure to the observed Landers aftershock sequence. The Landers mainshock occurred on the 6/28/1992 and its epicenter was located at longitude -116.44 and latitude 34.20 and a magnitude of 7.3. We analyzed the relocated earthquake catalog of Hauksson et al. (2003) for the region -117.5W to -115.5W and 33.25N to 35.5N and the time interval between $t_1=6/28/1991$ and $t_2=6/28/1993$ (SCEDC webpage at <http://www.data.scec.org/research/altcatalogs.html>).

| model | 1 day after mainshock | | | 5 days after mainshock | | | 10 days after mainshock | | |
|-------|-----------------------|----------|------------|------------------------|----------|------------|-------------------------|----------|------------|
| | \bar{r} | r_{50} | σ_r | \bar{r} | r_{50} | σ_r | \bar{r} | r_{50} | σ_r |
| 1 | 0.88 | 0.89 | 0.02 | 0.94 | 0.94 | 0.02 | 0.94 | 0.94 | 0.02 |
| 2a | 0.85 | 0.86 | 0.05 | 0.92 | 0.94 | 0.07 | 0.92 | 0.94 | 0.06 |
| 2b | 0.89 | 0.90 | 0.05 | 0.93 | 0.95 | 0.07 | 0.93 | 0.95 | 0.06 |

Table 2: Linear correlation coefficient between the predicted and the true spatial probability distribution for the next 24 hours as a function of time after the mainshock: mean \bar{r} , median r_{50} , and standard deviation σ_r .

The ETAS parameters were inverted for $M \geq 3$ events after each 24 hours subsequent to the mainshock, i.e. at times $T_i = t_M + i$ days. However, the maximization of the log-likelihood function (Eq.3) was done only for aftershocks occurring after the first 12 hours (i.e. within $[t_M + 0.5, T_i]$) to account for possible incompleteness of the recordings in the first time interval (Kagan, 2004). We chose 12 hours in agreement with the estimation of Helmstetter et al. (2005) for the time of incompleteness for $M \geq 3$ in southern California. However, all earthquakes that occurred before $t_M + 0.5$ day (also foreshocks) were taken into account to calculate the rates at times larger than that. More precisely, the local rates defined by Eq.(1) were calculated from all preceding events (since 6/28/1991) whereas the log-likelihood function (Eq.3) was calculated only for the N events occurred in the time period $[t_M + 0.5, T_i]$. Table 3 shows the estimated parameters (mean and standard deviation of the 90 estimations with $T_i = 1, \dots, 90$ days) in comparison to the values of the background model. The background values were estimated from the seismic activity preceding the mainshock in the larger region -119W to -115.5W and 32.5N to 36.5N within the time interval between $t_1=1/1/1984$ and $t_2=6/27/1992$. In contrast to the estimates given in table 1, we also inverted the α -parameter from the data.

The parameter estimations differ significantly between the space-dependent and independent ETAS models. Similar to our synthetic study, the inverted K value is much higher and the α -value much smaller in the case of the space-time model than for the space-independent model, whereas the c and p -values are similar. The estimations are stable after approximately 4 days after the mainshock, however, they are not always similar to the pre-mainshock values. In particular the c -value for the Landers sequence is larger than that estimated from the preceding seismicity. The α -parameter values for the background seismicity and Landers aftershocks are also significantly different. However, both α -values inverted by the space-independent model are now in good agreement with the range of estimations resulting from direct fits (Helmstetter, 2003; Helmstetter et al., 2005). Furthermore, it is interesting to note that the q -value is close to 1.5 for both data sets. This corresponds to a decay with distance according to $\sim r^{-3}$. Thus our result indicates that aftershocks around the fault zone seem to be triggered by static rather than, as recently claimed, by dynamic stress changes (Felzer and Brodsky, 2006).

Finally, we tested the forecasting ability for both models. In the same way as described for the synthetic simulations (see Section 2), we forecasted the number of $M \geq 3$ -earthquakes in the next 24 hours based on the aftershocks that already occurred. For the simulation-based forecasts, we used a maximum aftershock magnitude of 6.3 to stabilize the forecasts by avoiding that one simulation, which consists of a very large aftershock triggering a huge number of secondary events, can dominate the ensemble forecast. Similar results are obtained for the median value in the case of an unrestricted maximum magnitude. The b -value for the simulations was estimated at each time step T_i from the preceding aftershock activity by the maximum likelihood method (Aki, 1965) yielding values between 0.89 and 0.94. In addition to the previous models, we also calculated

| | space-independent model | | space-dependent model | |
|------------|-------------------------|------------|-----------------------|------------|
| | aftershocks | background | aftershocks | background |
| K | 0.0067 ± 0.0022 | 0.021 | 0.097 ± 0.026 | 0.040 |
| c [days] | 0.013 ± 0.038 | 0.003 | 0.029 ± 0.028 | 0.001 |
| α | 0.99 ± 0.05 | 0.70 | 0.24 ± 0.03 | 0.36 |
| p | 1.07 ± 0.15 | 1.05 | 1.05 ± 0.11 | 0.98 |
| q | - | - | 1.49 ± 0.02 | 1.44 |
| d [km] | - | - | 0.50 ± 0.06 | 0.48 |

Table 3: The estimated ETAS-parameters for the background and Landers aftershock activity. The latter are estimated with their standard deviations from the time intervals $[0.5, T_n]$ days with $T_n=1, 2, \dots, 90$ days.

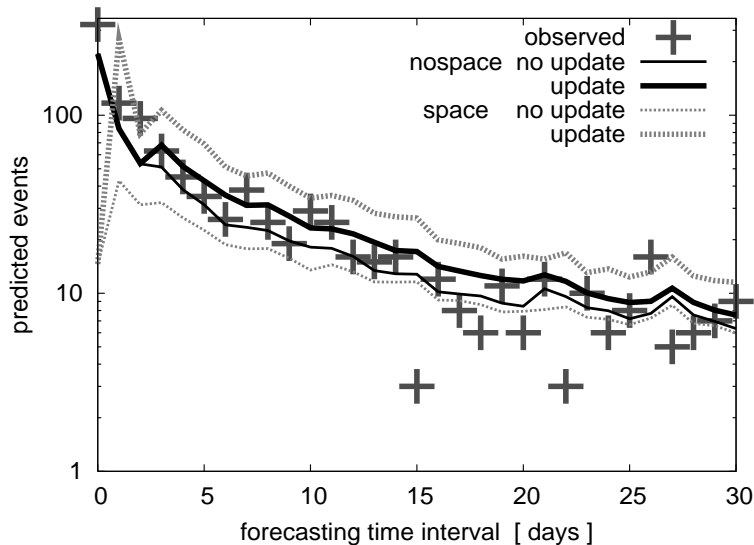


Figure 4: The forecasted number of $M \geq 3$ aftershocks within the next 24 hours as a function of time after the Landers mainshock. The crosses indicate the observed numbers of events and the different curves refer to the different forecasting procedures.

the forecasts based on the background models, that is, for the case that the parameters were not updated during the ongoing aftershock sequence. The resulting forecasts are shown in Fig. 4 where they are compared with the observations. It is obvious that the space-independent ETAS model best predicts - at least in the first days - the occurred rates; in particular the forecast based on updated parameters performs the best. On the other hand, the space-time ETAS model leads to significantly biased estimations. The background model clearly under-predicts and the updated version over-predicts the real aftershock numbers. Please note that a more detailed comparative test of the spatiotemporal forecasts for the Landers aftershock sequence will be done in a forthcoming paper.

4 Summary and Conclusions

The ETAS model is a very powerful model in describing short-time clustering of earthquakes. Here we show, however, that the estimations of the space-time ETAS model can be strongly biased if

earthquakes are treated as point-sources with spatially isotropic aftershock probability. In principle, anisotropic aftershock distributions can be considered in the space-time ETAS model, e.g. by an ellipsoidal instead of a radial distribution (Ogata, 1988; Schoenberg, 2003; Ogata and Zhuang, 2006). However, this requires additional assumptions and a non-trivial fit to the aftershock distribution. Therefore, the anisotropy is often neglected, which explains why the scaling parameter α for the aftershock productivity is generally found to be significantly smaller if it is estimated by a space-dependent point-process model rather than by stacking procedures. Using synthetic aftershock sequences and the test case of the Landers sequence, we have demonstrated that neglecting this problem can lead to a drastic drop of the forecasting ability of the ETAS model. As a result of our study, we propose an optimized strategy for using the ETAS model for earthquake forecasting: (1) forecast of the number of events by means of applying the space-independent ETAS model to a region surrounding the mainshock (in order to invert for K, c, α, p), (2) estimate the spatial probability distribution based on the estimation of the space-time model. In the future, we will compare this procedure to alternative model forecasts and test the forecasts for a number of different aftershock sequences.

Acknowledgments

This work is part of the EU-SAFER project (contract 036935). We are grateful to the associate editor Stefan Wiemer and an anonymous referee for the detailed report and helpful recommendations. Finally we are thankful to Jochen Woessner for stimulating this research by his forecasting tests.

References

- Aki, K. (1965). Maximum likelihood estimate of b in the formula $\log N = a - bM$ and its confidence limits, *Bull. Earthquake Res. Inst.* 43, 237–239.
- Christophersen, A., and Smith, E.G.C. (2008). Foreshock rates from aftershock abundance with different search algorithms, *Bull. Seismol. Soc. Am.*, in review.
- Console R., M. Murru, and A.M. Lombardi (2003). Refining earthquake clustering models, *J. Geophys. Res.*, 108(B10), 2468, doi:10.1029/2002JB002130.
- Console R., M. Murru, F. Catalli, and G. Falcone (2006). Real time forecasts through an earthquake clustering model constrained by the rate-and-state constitutive law: Comparison with a purely stochastic ETAS model, *Seism. Res. Lett.*, 78, 49–56.
- Daley, D.J., and D. Vere-Jones (2003). *An Introduction to the Theory of Point Processes, Volume I: Elementary Theory and Methods*, 2nd ed., Springer.
- Felzer, K.R., and E.E. Brodsky (2006). Decay of aftershock density with distance indicates triggering by dynamic stress, *Nature*, 441 (7094), 735–738.
- Felzer, K.R., T.W. Becker, R.E. Abercrombie, G. Ekstrom, and J.R. Rice (2002). Triggering of the 1999 M-W 7.1 Hector Mine earthquake by aftershocks of the 1992 M-W 7.3 Landers earthquake,

J. Geophys. Res., 107 (B9), 2190.

Felzer, K.R., R.E. Abercrombie, and G. Ekstrom (2004). A common origin for aftershocks, foreshocks, and multiplets, *Bull. Seismol. Soc. Am.*, 94 (1), 88–98.

Fletcher, R., and M.J.D. Powell (1963). A rapidly convergent descent method for minimization, *Comput. J.*, 6, 163–168.

Gerstenberger, M.C., S. Wiemer, L. M. Jones, and P. A. Reasenber (2005). Real-time forecasts of tomorrow's earthquakes in California, *Nature*, 435, 328–331.

Hauksson, E., W-C. Chi, and P. Shearer (2003). Comprehensive waveform cross-correlation of southern California seismograms: Part 1. Refined hypocenters obtained using the double-difference method and tectonic implications (abstract), *Fall. Ann. Meeting, American Geophys. Un.*, Dec. 8-12, 2003, San Francisco CA.

Helmstetter, A. (2003). Is earthquake triggering driven by small earthquakes? *Phys. Rev. Lett.*, 91 (5), 058501.

Helmstetter A., and D. Sornette (2002). Subcritical and supercritical regimes in epidemic models of earthquake aftershocks, *J. Geophys. Res.*, 107(B10), 2237.

Helmstetter, A., D. Sornette, and J.-R. Grasso (2003). Mainshocks are aftershocks of conditional foreshocks: How do foreshock statistical properties emerge from aftershock laws, *J. Geophys. Res.*, 108 (B1), 2046.

Helmstetter, A., Y.Y. Kagan, and D.D. Jackson (2005). Importance of small earthquakes for stress transfers and earthquake triggering, *J. Geophys. Res.*, 110, B05S08, doi:1029/2004JB003286.

Helmstetter, A., Y.Y. Kagan, and D.D. Jackson (2006). Comparison of short-term and time-independent earthquake forecast models for southern California, *Bull. Seismol. Soc. Am.*, 96 (1), 90–106.

Helmstetter, A., Y.Y. Kagan, and D.D. Jackson (2007). High-resolution time-independent grid-based forecast for $M \geq 5$ earthquakes in California, *Seism. Res. Lett.*, 78, 78-86.

Hough, S.E., and K.B. Olsen (editors) (2007). Special issue on: Regional Earthquake Likelihood Models, *Seismol. Res. Lett.*, 78, 7-140.

Kagan, Y.Y. (2004). Short-term properties of earthquake catalogs and models of earthquake source, *Bull. Seismol. Soc. Am.*, 94 (4), 1207–1228.

Kanamori, H., and D.L. Anderson (1975). Theoretical basis of some empirical relations in seismology, *Bull. Seismol. Soc. Am.*, 65 (5), 1073–1095.

Ogata, Y. (1988). Statistical models for earthquake occurrence and residual analysis for point processes, *J. Am. Stat. Assoc.*, 83, 9–27.

Ogata, Y. (1992). Detection of precursory relative quiescence before great earthquakes through a

statistical model, *J. Geophys. Res.*, *97*, 19,845–19,871.

Ogata, Y. (1998). Space-time point-process models for earthquake occurrences, *Ann. Inst. Statist. Math.*, *50*, 379–402.

Ogata, Y., and H.C. Zhuang (2006). Space-time ETAS models and an improved extension, *Tectonophysics*, *413* 13–23.

Schoenberg, F.P. (2003). Multidimensional residual analysis of point process models for earthquake occurrences, *J. Am. Stat. Assoc.*, *98*, 789–795.

Utsu, T., Y. Ogata, and R.S. Matsu'ura (1995). The centenary of the Omori formula for a decay of aftershock activity, *J. Phys. Earth*, *43*, 1–33.

Utsu, T., and A. Seki (1955). Relation between the area of aftershock region and the energy of the main shock (in Japanese), *J. Seismol. Soc. Jpn.*, *7*, 233–240.

Wells, D. L., and K.J. Coppersmith (1994). New empirical relationships among magnitude, rupture length, rupture width, rupture area, and surface displacement, *Bull. Seismol. Soc. Am.*, *84*, 974–1002.

Yamanaka, Y., and K. Shimazaki (1990). Scaling relationship between the number of aftershocks and the size of the main shock, *J. Phys. Earth*, *38* (4), 305–324.

Zhuang, J., Y. Ogata, and D. Vere-Jones (2004). Analyzing earthquake clustering features by using stochastic reconstruction, *J. Geophys. Res.*, *109* (B5), B05301.

Zhuang, J.C., C.P. Chang, Y. Ogata, and Y.I. Chen (2005). A study on the background and clustering seismicity in the Taiwan region by using point process models, *J. Geophys. Res.*, *110* (B5), B05S18.